Commun. Comput. Phys.
doi: 10.4208/cicp.OA-2016-0068

Vol. **21**, No. 4, pp. 1154-1172
April 2017

Calculation of Resonance S-Matrix Poles by Means of Analytic Continuation in the Coupling Constant

Jiří Horáček[1,*] and Lukáš Pichl[2]

[1] *Charles University, Faculty of Mathematics and Physics, Prague, Czech Republic.*
[2] *International Christian University, 3-10-2 Osawa, Mitaka, Tokyo 181-8585, Japan.*

Received 12 May 2016; Accepted (in revised version) 4 September 2016

Abstract. The method of analytic continuation in the coupling constant in combination with the use of statistical Padé approximation is applied to the determination of complex S-matrix poles, i.e. to the determination of resonance energy and widths. These parameters are of vital importance in many physical, chemical and biological processes. It is shown that an alternative to the method of analytic continuation in the coupling constant exists which in principle makes it possible to locate several resonances at once, in contrast to the original method which yields parameters of only one resonance. In addition the new approach appears to be less sensitive to the choice of the perturbation interaction used for the analytical continuation than the original method. In this paper both approaches are compared and tested for model analytic separable potential. It is shown that the new variant of the method of analytic continuation in the coupling constant is more robust and efficient than the original method and yields reasonable results even for data of limited accuracy.

PACS: 31.15.-p

Key words: Analytical continuation in the coupling constant, resonance parameters, complex energy, statistical Padé approximation.

1 Introduction

Resonances defined as complex poles of the S-matrix [1] play an essential role in many areas of physics, chemistry, astronomy, biology, etc. The reason is that the presence of a resonance may increase the rate of a dynamical process by many orders of magnitude and in fact make it the dominant process. Let us mention for example the atomic processes controlling formation of stars and galaxies [2], radiation damage in biological tissues [3], formation of metastable long-lived states in molecular hydrogen [4], etc.

---

[*] Corresponding author. *Email addresses:* `jiri.horacek@mff.cuni.cz` (J. Horáček), `lukas@icu.ac.jp` (L. Pichl)

There exist several methods for the determination of resonance parameters (i.e. the real and imaginary part of the complex energy of the S-matrix pole). Let us mention just a few of them: stabilisation methods [5–7], Stieltjes imaging techniques [6], complex rotation [8,9], complex absorbing potential [10,11], etc. All the methods are computationally demanding requiring usually the use of complex arithmetics. The method of analytic continuation in the coupling constant represents the less computationally demanding method which uses real arithmetics only. This is a very important fact because for the determination of resonances of extended many electron systems which are essential in various biological and chemical processes (for example radiation damage of DNA) one has to use commercial quantum chemistry codes which are limited to real arithmetics only. The method of analytic continuation in coupling constant (ACCC) has been introduced in nuclear physics by Krasnopolsky and Kukulin [12,13] and is described in detail in the monograph [1]. The ACCC approach has found several applications mainly in nuclear physics, see e.g. [14–18]. Recently Horáček et al. [19] and Papp et al. [20] have applied the ACCC method to real molecular resonances, discussing the $^2\Pi_g$ state of N_2^- resonance of molecular nitrogen and resonance of amino acid molecules (alanine, glycine and valine). In addition Horáček, Paidarová and Čurík applied a modification of the ACCC method to the determination of resonance energy and width of the $^2B_{2g}$ shape resonance of ethylene [21] and diacetylene [22] proving that the ACCC method can yield accurate resonance energies and widths for non-model situations based on data obtained by using standard quantum chemistry codes. It therefore seems worthwhile to study the properties and numerical efficiency of the method in order to get a deeper insight into its properties. One of the open questions is the right selection of the perturbation interaction; this problem seems to be of crucial importance. It is the purpose of this work to propose a new form of the ACCC method, to test the role and choice of the perturbation potential and to compare the numerical efficiency of both approaches. In what follows we shall use units $\hbar=1$ and $m=\frac{1}{2}$ unless explicitly stated.

2 Description of resonances

In its simplest form (i.e. one dimensional radial problem) the resonances are defined as solutions of the following integro-differential Schrödinger equation

$$-\frac{d^2\psi_l(r)}{dr^2}+V(r)\psi_l(r)+\frac{l(l+1)}{r^2}\psi_l(r)+\int_0^\infty W(r,r^{'})\psi_l(r^{'})dr^{'}=k^2\psi_l(r) \tag{2.1}$$

satisfying the boundary conditions of Siegert [27]

$$\psi_l(0)=0, \qquad \frac{\psi_l^{'}(R)}{\psi_l(R)}=ik', \tag{2.2}$$

where R is a distant point at which the interaction V and W is negligible and l is the angular momentum of the resonance. For realistic molecular resonance the equation is of course multidimensional. The term $V(r)$ stands for the local interaction, whereas $W(r,r')$ denotes the nonlocal interaction term. The number of independent variables is typically several tens up to hundreds. It is important to stress that the sought after eigenvalue k is complex and in addition it appears in the boundary condition Eq. (2.2). This combination makes the eigenvalue problem Eq. (2.1) nonlinear. Of physical importance is the quantity $\mathrm{E}_R = \mathrm{Re(k)}^2 - \mathrm{Im(k)}^2$ which represents the energy of the resonance and $\Gamma = 4\mathrm{Re(k)Im(k)}$ its width.

3 Analytic continuation in the coupling constant

To calculate the bound state energies and their square integrable wave functions is now a routine task even for large polyatomic molecules and many commercial programs are available. The calculation of resonance energy and width is however a serious problem [8] whereas bound state energy calculations is easy. It is therefore natural to ask whether one can obtain the resonance energy and perhaps even its width from a knowledge of the bound state energies alone. This really can be done in several more or less accurate ways, see for example [23]. Here we describe one method which is able to provide the resonance energy and also the resonance width to a high degree of accuracy, the method of analytical continuation in the coupling constant (ACCC). The ACCC method works as follows [1]: let us for simplicity assume that motion of the electron in the vicinity of a molecule is determined by a Hamiltonian H which generates a resonance at a complex energy E

$$E = E_R - \frac{i}{2}\Gamma,$$

where E_R is the resonance energy and Γ is the resonance width. Let us now add an attractive short-range interaction U to the original Hamiltonian H multiplied by a real positive parameter λ

$$H \to H + \lambda U. \tag{3.1}$$

At increasing λ the new Hamiltonian H gets more attractive and some resonance states eventually transform into bound states. At such values of λ the bound state energies $E(\lambda)$ may be easily obtained. The problem now stands how to find from the knowledge of $E(\lambda)$ calculated in the bound state region the complex quantity $E(\lambda=0)$. All calculated $E(\lambda)$ values are real and any extrapolation must yield real value only whereas to find the resonance parameters we must determine a complex number. It is shown in [1] that a naive extrapolation of energy in λ, $E \approx E_0 + E_1\lambda + E_2\lambda^2\cdots$, sometimes used in quantum chemistry is not sufficient to get both the resonance energy and the resonance width and that the extrapolations should be replaced by an analytic continuation. In addition the parameter used for the continuation is not the parameter λ itself but a new variable $y = \sqrt{\lambda - \lambda_0}$ which will be discussed below. The function to be analytically continued is the momentum $k(\lambda(y))$, $\hbar^2 k^2/2m = E$ where m is the reduced mass. This is the most essential ingredient of the ACCC method.

In this work we will carry out the analytic continuation by using the so called statistical Padé approximation (Padé III approximation) [1]. This approach has several advantages:

1. It allows to use low-order Padé approximations even if a large number of points are available.
2. It allows us to take into account the inaccuracy of the input data.
3. It can describe a much broader range of functions: for example functions with poles and cuts.
4. It carries out the analytical continuation automatically [1], etc.

Since an absolute majority of molecular resonances possesses nonzero angular momentum l we will consider here the ACCC method for $l \neq 0$. For $l=0$ the situation is more complicated and will not be discussed here. As has already been shown (see e.g. [1]), at small values of k the function $k(\lambda)$ behaves as $k(\lambda) \approx a\sqrt{\lambda-\lambda_0}$ where λ_0 denotes the point $k(\lambda_0)=0$. At smaller values of $\lambda < \lambda_0$, $k(\lambda)$ therefore becomes complex and the resonance energy acquires its imaginary part.

3.1 ACCC algorithm

The ACCC calculation proceeds as follows:

- Bound state energies E_i are calculated for several values of the parameter λ_i using standard quantum chemistry codes and input data $\{\kappa_i(\kappa_i=-ik_i),\ \lambda_i,\ i=1,2,\cdots,L\}$ are generated ($\hbar^2 k_i^2/2m=E_i$). This step represents a routine task.
- Based on the input data the Padé approximation $\lambda(\kappa) \approx \frac{P_N(\kappa)}{Q_M(\kappa)}$, is constructed and evaluated at $\kappa=0$. In this way the bifurcation point λ_0 is found.
- Then the second Padé approximation $\kappa(\lambda) \approx \frac{P_N(\sqrt{\lambda-\lambda_0})}{Q_M(\sqrt{\lambda-\lambda_0})}$ is constructed and evaluated at λ=0 and the resonance parameters thus determined

$$k_1+ik_2=k^{[N/M]} \quad (\lambda=0), \tag{3.2}$$

$$E_R=(k_1^2-k_2^2)\hbar^2/2m, \qquad \Gamma=2k_1k_2\hbar^2/m. \tag{3.3}$$

3.2 Inverse ACCC algorithm

The standard ACCC method is in fact a two-step method requiring two fits. First the bifurcation point is determined and then by the second fit the resonance energy and width is computed. It is observed that the final value of the resonance parameters is very sensitive to the precise value of the bifurcation point λ_0. Even minor changes of its value may lead to significant changes of the obtained resonance parameters. There is however another much simpler approach which requires only one function to be fitted. This approach is based on the analytical continuation of the function $\lambda(\kappa)$ (the inverse function to the function $\kappa(\lambda)$). For this reason we will call the new approach the inverse ACCC method (IACCC). Let us start from the first fit of the ACCC method

$$\lambda(\kappa) \approx \frac{P_N(\kappa)}{Q_M(\kappa)}. \tag{3.4}$$

Then the resonance parameters may be obtained by solving the simple polynomial equation

$$P_N(\kappa) = 0. \tag{3.5}$$

The bifurcation point $\lambda_0 = P_N(0)$. Resonances are determined directly as the physical roots of P_N. In addition this approach may in principle be able to determine positions of virtual states and of other resonances because solving Eq. (3.5) provides us with N solutions. The standard ACCC method allows for determination of only one resonance which is connected with the bound state region through the origin. An open question remains the stability of this approach. It is well known that determination of polynomial roots is a very sensitive problem. A variant of the IACCC was proposed in [22]. In the following we compare the basic properties of both ACCC and IACCC approaches.

4 Model potential

As a model potential for the study of the numerical performance of both methods we use the separable interaction

$$U(r,r') = \sum g_i(r) g_i(r'). \tag{4.1}$$

In what follows the local term is set as $V(r) = 0$, which is consistent with the fact that separable interactions represent at low energies good description of local short range interactions.

This type of interaction is often used for the description of nuclear forces or effective interactions in atomic, molecular physics and other fields [24–26] and greatly simplifies solution of Eq. (2.1). The Schrödinger equation then reads

$$\frac{d^2\psi_l(r)}{dr^2} + \frac{l(l+1)}{r^2}\psi_l(r) + \sum g_i(r) \int_0^\infty g_i(r')\psi_l(r')dr' = k^2\psi_l(r). \tag{4.2}$$

To convert the resonance states into bound states the perturbation interaction must be attractive. If we choose the perturbation potential in the form (4.1) we can write application of the total Hamiltonian H_λ on a wave function $\psi(r)$ as

$$H_\lambda\psi(r) = H\psi(r) - \lambda\sum g_i(r) \int_0^\infty g_i(r')\psi(r')dr', \tag{4.3}$$

where H is the original unperturbed Hamiltonian and the perturbation is of an attractive nature for $\lambda \geq 0$.

The projective nature of the perturbation allows for an explicit determination of the coupling parameter $\lambda(\kappa)$ as a function of κ, $k=i\kappa$, $E=-\kappa^2$ [28]. For one term perturbation potential and for $H=H_0$ where H_0 denotes the free Hamiltonian we get

$$\lambda(\kappa)=-\frac{1}{\int dr\int dr' g(r)G(r,r',-\kappa^2)g(r')}, \tag{4.4}$$

where $G(r,r',k)$ is the Green's function of the unperturbed problem. The behavior of $\lambda(\kappa)$ has been studied in detail only for the partial wave $l=0$ in [28]. Since most of the atomic and molecular resonances are formed by centrifugal repulsive interaction we will consider the partial wave $l=1$ as representative of all nonzero angular momentum partial waves. In accordance with the nomenclature in scattering theory we represent the function $g(r)$, the so-called form factor, in the form

$$g(r)=\sqrt{\frac{\pi}{2}}\int_0^\infty g(p)j_l(pr)p\,dp, \tag{4.5}$$

where $j_l(x)$ is the spherical Bessel function.

To start with we choose the form factor $g(p)$ in the form proposed by Mongan [24]

$$g(p)=\frac{p}{p^2+\alpha^2} \tag{4.6}$$

which fulfils the threshold law [24]

$$g_l(p)\sim p^l, \quad \text{for} \quad p\to 0. \tag{4.7}$$

For this potential we get

$$\lambda(\kappa)=\frac{4}{\pi}\frac{(\alpha+\kappa)^2}{\alpha+2\kappa}. \tag{4.8}$$

Solving this equation for κ gives two solutions

$$\kappa_{1,2}=\mu-\alpha\pm\sqrt{\mu(\mu-\alpha)}, \tag{4.9}$$

where $\mu=\frac{\pi\lambda}{4}$. It follows from this equation that the resonances (i.e. solutions with nonzero imaginary part) exist only in a narrow range of λ values

$$0<\frac{\pi\lambda}{4}<\alpha. \tag{4.10}$$

Outside this range both solutions are real and represent a pair of one bound and one virtual state or two virtual states. For $\lambda>\frac{4\alpha}{\pi}$ we have one bound state which moves from zero to infinity at increasing λ and one virtual state which moves from zero to $-\frac{\alpha}{2}$. For negative λ we have two virtual states originating at $\kappa=-\alpha$, one moves towards $-\frac{\alpha}{2}$,

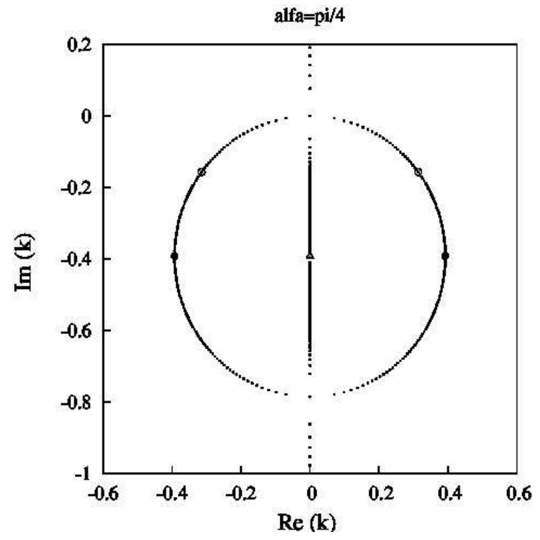

Figure 1: Trajectory of resonance poles $k=k_1+ik_2$ for single separable term (4.1) with the formfactor (4.6) for $\alpha=\frac{\pi}{4}$ in dependence on the coupling parameter λ. The triangle denotes the pole of the function $\lambda(\kappa)$ located at $\kappa=-\frac{\alpha}{2}$. The open and full circles indicate positions of the resonances at $\mu=\frac{3\alpha}{4}$ and $\mu=\frac{\alpha}{2}$, respectively.

the other to $-\infty$. The resonances are limited to a circle of radius $\frac{\alpha}{2}$ centered at $-\frac{\alpha}{2}$. The function $\kappa(\lambda)$ has thus two square-root-type singularities, one at $\lambda=\frac{4\alpha}{\pi}$, the other at $\lambda=0$.

In addition there is one pole at $\kappa=-\frac{\alpha}{2}$. This finite value of κ can be reached only for $\lambda\to\pm\infty$. For $\mu=\frac{\alpha}{2}$ the resonance is located at $k=\pm\frac{\pi}{8}-i\frac{\pi}{8}$, see Fig. 1 showing the trajectory of $k(\lambda)$ where this resonance is denoted by the solid circles. This choice represents an extreme case: the resonance energy $E_R=0$ whereas the width $\Gamma=\alpha^2$. A physically relevant resonance (i.e. $E>0$ and $\Gamma<E$) obtained with $\mu=\frac{3\alpha}{4}$ is denoted by open circles in Fig. 1.

To describe a more realistic case to which both the ACCC and IACCC methods can be applied we use the interaction consisting of two separable terms

$$V\psi=-\lambda_1 g_\alpha(r)\int g_\alpha(r')\psi(r')dr'-\lambda_2 g_\beta(r)\int g_\beta(r')\psi(r')dr' \tag{4.11}$$

with

$$g_\alpha(p)=\frac{p}{p^2+\alpha^2},\qquad g_\beta(p)=\frac{p}{p^2+\beta^2}. \tag{4.12}$$

The parameters λ_2 and β are chosen so as to form a resonance pair at $\kappa_R=\pm\kappa_1+\imath\kappa_2$ whereas the parameter λ_1 has been varied as the coupling constant in the ACCC method. For $\lambda_1=0$ the resonance should be obtained. Solving Eq. (4.2) with the potential (4.11) and (4.12) leads to

$$\lambda_1(\kappa)=\frac{4(\alpha+\beta)^2(\alpha+\kappa)^2[\lambda_2\pi(\beta+2\kappa)-4(\beta+\kappa)^2]}{\pi[\lambda_2\pi(\alpha-\beta)^2(\alpha\beta+2\alpha\kappa+2\beta\kappa)-4(\alpha+\beta)^2(\beta+\kappa)^2(\alpha+2\kappa)]}. \tag{4.13}$$

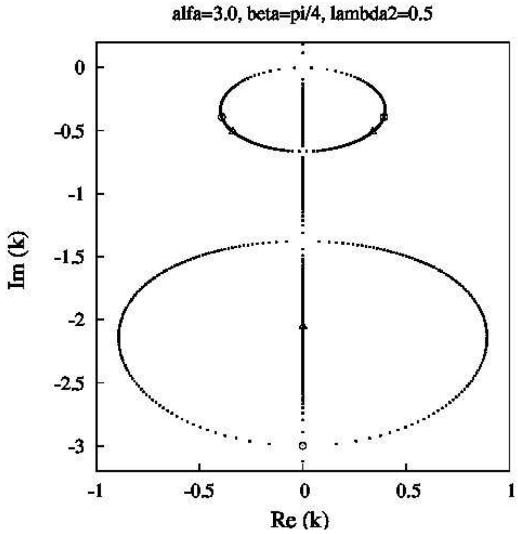

Figure 2: Trajectories of the resonance (virtual and bound states) as functions of the parameter λ_1 for the potential (4.11) and (4.12) consisting of two separable terms. In this figure $\alpha=3.0$, $\beta=\frac{\pi}{4}$ and $\lambda_2=0.5$.

The trajectory of κ as function λ_1 now gets more complicated. $\lambda_1(\kappa)$ is given in the form of a ratio of two polynomials $P(\kappa)$ and $Q(\kappa)$, Eq. (4.13)

$$\lambda_1(\kappa)=\frac{P(\kappa)}{Q(\kappa)} \tag{4.14}$$

of the order 4 and 3 respectively. Hence we will have four solutions of the equation

$$P(\kappa)=0 \tag{4.15}$$

and the function $\lambda_1(\kappa)$ will possess three poles. According to Eq. (4.13) $P(\kappa)$ has one root of the second order at $\kappa=-\alpha$. This root is related to the perturbation potential only and has no physical relevance. The other roots of $P(\kappa)$ determine the position of the resonance. The crucial question now is how does the trajectory depend on the parameter α determining the perturbation used for the process of analytic continuation. In Fig. 2 we plot the trajectories of the resonance roots of $P(\kappa)$ for $\alpha=3.0$, $\beta=\frac{\pi}{4}$, $\lambda_2=0.5$. This is the extreme case of resonance mentioned above. Physically relevant resonances are located closer to the origin. The resonance is now located on the outer curve as indicated by the open circles. The trajectories now consist of two loops; one adjacent to the origin the other not. At reducing α the loops approach each other, see Fig. 3 for $\alpha=1.0$ and Fig. 4 for $\alpha=0.5$. At further reducing the value of α the loops interchange their positions and the resonance is eventually located on the lower loop, see Fig. 5 for $\alpha=0.1$.

For this choice of α the journey of the function $\kappa(\lambda)$ from positive values of κ corresponding to the bound states to the resonance represents a very complicated trajectory

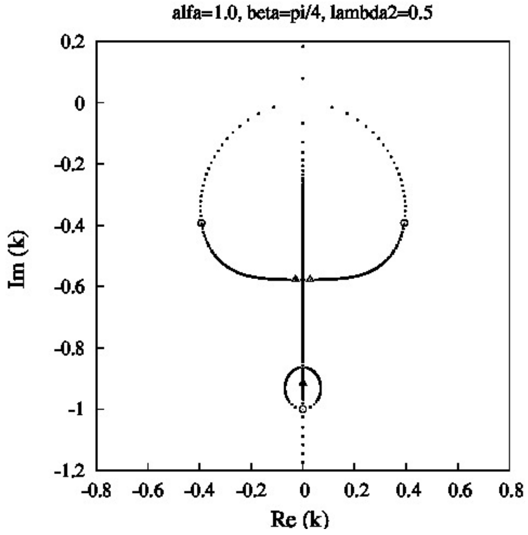

Figure 3: The same as Fig. 2 but for $\alpha = 1.0$.

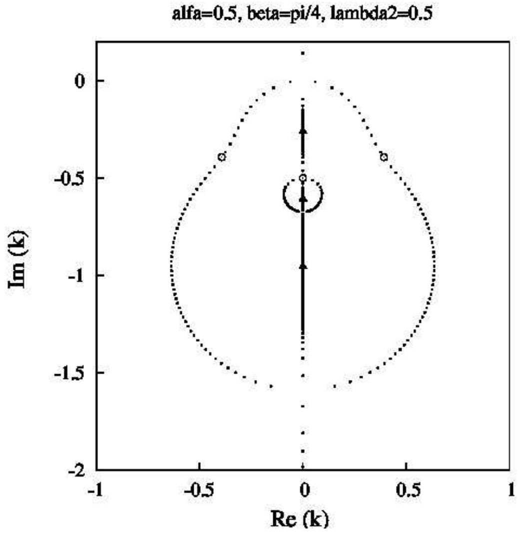

Figure 4: The same as Fig. 2 but for $\alpha = 0.5$.

and it is expected that the classical ACCC method may have serious problems to reach the resonance. It is obvious that to represent such a complicated behavior would require a very high order of Padé approximation. For the inverse method, however, this behavior represents no difficulty. This feature also indicates that the good choice of the perturbation potential is essential. Since, however, in real applications the underlying interaction is not known, one has to try to find the best choice by trial and error.

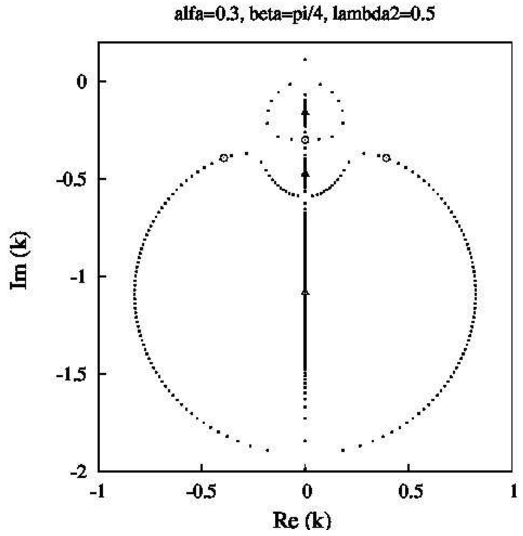

Figure 5: The same as Fig. 2 but for $\alpha=0.3$.

5 Determination of Padé approximants

Whereas Padé approximants of types I and II have been widely used in physics for many years [29–35] the number of applications of Padé approximants of type III (also known as statistical Padé approximants) has been much more limited, and most of these applications have been developed relatively recently.

The type-III Padé approximant of order $[N,M]$ representing a set of empirical values $f_i\,(i=1,\cdots,J)$ of a function $f(x)$, measured at points x_i with statistical errors ε_i, is defined as the rational function $P_N(x)/Q_M(x)$, where

$$P_N(x)=\sum_{j=0}^{N} p_j x^j, \qquad Q_M(x)=1+\sum_{k=1}^{M} q_k x^k \tag{5.1}$$

are polynomials of degrees N and M, respectively (with $M+N<J-1$), which minimizes the functional

$$\chi^2=\sum_{l=1}^{J}\left[\frac{P_N(x_l)}{Q_M(x_l)}-f_l\right]^2. \tag{5.2}$$

Unlike the approximants of types I and II, Padé approximants of type III allow for the finite accuracy of the data used for their construction. Accordingly, they provide a more suitable representation of empirically determined physical quantities.

However, the wider application of type-III Padé approximants has been hindered by the nonlinearity of the equations that must be solved for direct determination of the minimum of χ^2 in a least-squares fit. Moreover, the χ^2 surface may have complicated structure in the parameter space, with a large number of local minima, so that a numerical search procedure starting from a given point in parameter space does not necessarily lead to the global minimum. To overcome the problem of minimization of such complicated functions, several authors, see for example [32] have proposed iterative methods which reduce the original nonlinear problem of minimization of χ^2 to a succession of more tractable problems of solving a set of linear algebraic equations in each step. So far, no sufficient conditions for the convergence of these methods are known.

The basic problem is to find the sets of coefficients p_j and q_k in (5.2) which minimize the χ^2 functional (5.2). For this, we set the partial derivative of χ^2 with respect to each of the coefficients equal to zero:

$$\frac{\partial \chi^2}{\partial p_j}=0 \quad (j=0,1,\cdots,N), \qquad \frac{\partial \chi^2}{\partial q_k}=0 \quad (k=1,2,\cdots,M). \tag{5.3}$$

This leads to the set of equations

$$\sum_{J=0}^{N} H_{lj} p_j - \sum_{k=1}^{M} K_{lk} q_k = K_{l0} \quad (l=0,1,\cdots,N), \tag{5.4}$$

$$-\sum_{J=0}^{N} L_{mj} p_j + \sum_{k=1}^{M} M_{mk} q_k = -M_{m0} \quad (m=1,2,\cdots,M), \tag{5.5}$$

where

$$H_{ij}=\sum_{i=1}^{J} \frac{x_i^{i+j}}{Z_i^2}, \tag{5.6}$$

$$K_{lk}=\sum_{i=1}^{J} \frac{f_i x_i^{l+k}}{Z_i^2}, \tag{5.7}$$

$$L_{mj}=\sum_{i=1}^{J} \frac{P_N(x_i) x^{m+j}}{Q_M(x_l) Z_l^2}, \tag{5.8}$$

$$M_{mk}=\sum_{i=1}^{J} \frac{P_N(x_i) f_i x_i^{m+k}}{Q_M(x_i) Z_i^2}, \tag{5.9}$$

$$Z_i = Q_M(x_i). \tag{5.10}$$

Eqs. (5.4) and (5.5) are nonlinear in the unknown coefficients p_j and q_k, since these coefficients occur in the quantities H_{lj}, K_{lk}, L_{mj} and M_{mk}.

There are various methods linearizing the nonlinear equations, see e.g. [32]. Here we will follow the method [25] which consists of replacing the unknown values of $P_N(x_l)/Q_M(x_l)$ in the definitions of L_{mj} and M_{mk} by a linear combination of the previously computed values. Again we obtain an approximation to all the coefficients p_j and q_k in a single step by solving a set of linear equations.

6 Numerical tests

In this Section, we compare the numerical efficiency of both the ACCC and IACCC approaches. In addition we will try to find some hints how to choose the perturbative potential. In the original applications of the ACCC method to molecular resonances there was no possibility to change the parameters of the perturbative potential; the only choice was the Coulomb potential. Nowadays however short range perturbations may be incorporated into standard quantum chemistry codes and the problem how to choose the perturbative interaction deserves attention. To test the sensitivity of the ACCC method to the choice of the perturbative potential, here the parameter α in Eq. (4.6), we carried out calculations of the real and imaginary parts of the resonance position for $\beta=\pi$ and λ_2 = 3.8 using both the ACCC and the IACCC approaches. The calculations were done for three choices of α:

1. $\alpha=8.0$; the perturbative potential is in this case of much shorter range than the original potential $\beta=\pi$;

2. The choice $\alpha=4.0$ which is close to the potential generating the resonance and finally,

3. a potential of much longer range with $\alpha=0.1$. All the calculations were done using the double precision accuracy. For the model potential in Eqs. (4.11) and (4.12) we choose 100 points κ_i, $\kappa_i=\kappa_o+ih$ with $h=0.01$ and $\kappa_o=6h$ and calculate the corresponding values λ_i.

As Eq. (4.13) suggests at large values of κ, $\lambda(\kappa)$ behaves as a linear function of κ. The same also holds for Coulomb potential, where the energy $E=\kappa^2\approx\lambda^2$. To keep our approximation as close as possible to the studied case, we limit ourselves to Padé approximations which fulfill this criterion. This means that the lowest approximation will be the 3/1 approximation and the higher ones will be 4/2,5/3,$\cdots$. For example for N=3 we have

$$\lambda^{[3/1]}(\kappa)=\frac{\lambda_0+\mu_1\kappa+\mu_2\kappa^2}{1+\mu_3\kappa} \tag{6.1}$$

and for the original ACCC method

$$\lambda_0=\lambda^{[3/1]}\quad(\kappa=0), \tag{6.2}$$

$$\kappa^{[3/1]}(\lambda)=\frac{p_1\sqrt{\lambda-\lambda_0}+p_2(\sqrt{\lambda-\lambda_0})^2+p_3(\sqrt{\lambda-\lambda_0})^3}{1+p_4\sqrt{\lambda-\lambda_0}}. \tag{6.3}$$

The convergence rate of both approaches for the potential parameters $\alpha=8.0,\beta=\pi$ and $\lambda_2=3.8$ are shown in Table 1. The convergence is rapid and already the 4/2 approximation is correct to four significant digits. The results for smaller $\alpha=4$ are even faster and more stable, see Table 2. However, if we choose α small $\alpha=0.1$, we find (see

Table 1: Calculation of the real and imaginary part of the resonance pole k for $\alpha=8.0$, $\beta=\pi$ and $\lambda_2=3.8$.

Method	ACCC	ACCC	IACCC	IACCC
Padé order N/M	Re (k)	Im (k)	Re (k)	Im (k)
3/1	0.683227	-0.157307	0.627490	-0.211979
4/2	0.684650	-0.157025	0.684669	-0.157066
5/3	0.684735	-0.157012	0.684680	-0.157079
6/4	0.684725	-0.156996	0.684694	-0.157075
7/5	0.684560	-0.157068	0.684696	-0.157076
8/6	0.685613	-0.156065	0.684711	-0.157081
9/7	0.672437	-0.166696	0.684714	-0.157107
Exact	0.684694	-0.157080	0.684694	-0.157080

Table 2: Calculation of the real and imaginary part of the resonance pole k for $\alpha=4.0$, $\beta=\pi$ and $\lambda_2=3.8$.

Method	ACCC	ACCC	IACCC	IACCC
Padé order N/M	Re (k)	Im (k)	Re (k)	Im (k)
3/1	0.683775	-0.157754	0.673108	-0.170714
4/2	0.684672	-0.157064	0.684693	-0.157079
5/3	0.684678	-0.157055	0.684694	-0.157080
6/4	0.684760	-0.157064	0.684694	-0.157080
7/5	0.684687	-0.157082	0.684696	-0.157081
8/6	0.684492	-0.157152	0.684747	-0.157070
9/7	0.684855	-0.156951	0.684484	-0.157006
Exact	0.684694	-0.157080	0.684694	-0.157080

Table 3: Calculation of the real and imaginary part of the resonance pole k for $\alpha=0.1$, $\beta=\pi$ and $\lambda_2=3.8$.

Method	ACCC	ACCC	IACCC	IACCC
Padé order N/M	Re (k)	Im (k)		
3/1	0.562201	-0.441700	0.677297	-0.354440
4/2	0.729859	0.029740	0.785465	-0.126171
5/3	0.603559	-0.135412	0.684694	-0.157080
6/4	0.741936	-0.184830	0.684694	-0.157080
7/5	0.398952	-0.398606	0.684695	-0.157081
8/6	0.431249	-0.329162	0.684690	-0.157077
9/7	0.407140	-0.316552	0.684559	-0.157087
Exact	0.684694	-0.157080	0.684694	-0.157080

Table 3) that the results obtained with the IACCC method keep their high accuracy and speed of convergence whereas the results obtained with the ACCC method rapidly lose their accuracy. This is clearly demonstrated in Table 4 which shows the results of the 5/3

Table 4: Relative error of the real and imaginary part of resonance position calculated by both methods for $\alpha = 8.0$, 4.0 and 0.1.

Method	ACCC	ACCC	IACCC	IACCC
Relative error	Re (k)	Im (k)	Re (k)	Im (k)
α				
8	0.000060	0.00043	0.000024	0.000006
4	0.000023	0.00016	<0.000001	<0.000001
0.1	0.12	0.14	<0.000001	<0.000001

Padé approximation for all three choices of α. These results indicate that a good choice of the perturbative potential is of vital importance. This study suggests that the best convergence is obtained for $\alpha = 4.0$ which is close to the potential generating the resonance $\beta = \pi$, i.e. the perturbative potential should be as close to the original potential as possible.

For smaller values of α the convergence of ACCC method gets worse. The reason for this behavior is the presence of poles in the function $\lambda(\kappa)$, Eq. (4.13). For $\alpha = 4$ this function has one real pole at $\kappa = -3.845$ and two complex conjugate poles at $(-2.219 \pm i0.685)$. At $\alpha = 0.1$ there are three real poles at $\kappa_1 = -0.0637, \kappa_2 = -0.209$ and $\kappa_3 = -6.060$. These poles are much closer to the origin and much closer to the resonance than in the case $\alpha = 4.0$. This is probably the reason for the bad convergence (or even divergence) of the ACCC method. In fact, if the choice of the perturbative potential is wrong the resonance may occur on the second loop, as shown in Fig. 5, which is disconnected from the bound state region. On the other hand if we choose α too big the minimum value of the coupling parameter λ_0 needed to convert the resonance into a bound state increases making the perturbation big in comparison with the potential generating the resonance. For $\alpha = 8.0$ the critical value is $\lambda_0 = 0.621578$ whereas for $\alpha = 0.1$ it is much smaller $\lambda_0 = 0.0389$. It is therefore necessary to find a compromise value between these two extremes to get the best convergence rate.

In all cases discussed above the inverse IACCC approach has no difficulty and a high accuracy is obtained even for the "bad choice" $\alpha = 0.1$.

7 Restricted accuracy

It is well known that methods using analytic continuations require very precise input data. For example, Chao et al. [36] in applying a stabilization method combined with an analytic continuation to complex stationary points found that it is necessary to have at least six significant figures of accuracy in the real energies in order to accurately characterize the resonances. It is extremely difficult to get outputs from quantum chemistry codes converged to six significant digits. Rather the accuracy of 3-4 digits seems more realistic. It is therefore worthwhile to study the properties of the presented method with respect to rather limited accuracy of the input data. As well known it is important to

Table 5: Calculation of the real and imaginary part of the resonance pole k for $\alpha = 4.0$, $\beta = \pi$ and $\lambda_2 = 3.8$ using Eq. (7.2).

Padé order N/M	Re (k)	Im (k)
3/1	0.685627	-0.168435
4/2	0.684693	-0.157080
5/3	0.684693	-0.157080
Exact	0.684694	-0.157080

include any known feature into the representation of the function to be continued to improve the stability and accuracy of the continuation. Here we have one important fact at hand:

According to [1,12,13] it is known that at $\kappa \to 0$

$$\lambda(\kappa) \approx \lambda_0 + \lambda_2 \kappa^2 + \cdots. \tag{7.1}$$

To incorporate this feature into the fit we may represent $\lambda^{[M/N]}$ as

$$\lambda_{\mathrm{Q}}^{[M/N]}(\kappa) = \frac{\lambda_0 + \lambda_1 \kappa^2 + \lambda_2 \kappa^3 + \lambda_3 \kappa^4 + \cdots}{1 + q_1 \kappa^2 + q_2 \kappa^3 + \cdots}. \tag{7.2}$$

This expression has the right asymptotic behavior at large values of κ for $M = N - 2$ and fulfills the condition of missing the linear term Eq. (7.1) at $\kappa \to 0$ where N and M represent the number of coefficient in the nominator and denominator of Eq. (7.2), respectively. The convergence rate of the approximation (7.1) is very fast, see Table 5. To test the sensitivity of the present approach to the accuracy of the data we artificially reduced the accuracy of the input data by rounding the calculated bound state energies to smaller number N of significant digits down to $N = 2$ and applied the approximation Eq. (7.2) at 3/1, 4/2 and 5/3 levels to data with decreasing number of significant digits. The results are summarized in Tables 6, 7 and 8. The left column represents the number of significant digits used for the process of analytic continuation, in the other columns the real and imaginary part of the S-matrix pole is shown. The calculation was done at $\alpha = 4.0$. These Tables demonstrate the unusual stability of the IACCC method. It is seen that to get three figures accuracy of the S-matrix pole (such high accuracy is seldom obtained in experimental data, see for example [19, 37]) it is sufficient to use data accurate to four significant digits easily obtainable from commercial quantum chemistry codes.

Let us remark at this point that a wealth of mathematical literature is available for the case of local interaction. Similar studies have been rigorously carried out, within a general scattering framework, see e.g. [38], where the reader is referred for rigorous analytic studies of Jost functions and S-matrices, generalized Levinsons theorem, partial wave expansions, Breit Wigner Ansatz, Fano parameters and the inverse problem. B. Simon [39] in "Resonances in n-body quantum systems with dilatation analytic potentials and the foundations of time-dependent perturbation theory" studied the method of analytic continuation in the coupling constant. In Ref. [39] Simon merges in detail the work on the

Table 6: 3/1 calculation of the real and imaginary part of the resonance pole k for $\alpha=4.0$ using Eq. (7.2) with the reduced accuracy of the input data. The first column indicates the number of significant digits used. $\beta=\pi$ and $\lambda_2=3.8$.

Number of digits	Re (k)	Im (k)
16	0.685627	-0.168435
8	0.685627	-0.168435
6	0.685627	-0.168435
5	0.685627	-0.168435
4	0.685850	-0.168185
3	0.683446	-0.170760
2	0.610814	-0.206855

Table 7: 4/2 calculation of the real and imaginary part of the resonance pole k for $\alpha=4.0$ using Eq. (7.2) with the reduced accuracy of the input data. The first column indicates the number of significant digits used. $\beta=\pi$ and $\lambda_2=3.8$.

Number of digits	Re (k)	Im (k)
16	0.684693	-0.157080
8	0.684693	-0.157080
6	0.684693	-0.157080
5	0.684693	-0.157080
4	0.683605	-0.155528
3	0.683262	-0.162309
2	0.648001	-0.223547

Table 8: 5/3 calculation of the real and imaginary part of the resonance pole k for $\alpha=4.0$ using Eq. (7.2) with the reduced accuracy of the input data. The first column indicates the number of significant digits used. $\beta=\pi$ and $\lambda_2=3.8$.

Number of digits	Re (k)	Im (k)
16	0.684693	-0.157080
8	0.684693	-0.157080
6	0.684693	-0.157080
5	0.684694	-0.157080
4	0.675128	-0.157612
3	0.669916	-0.160521
2	0.673762	-0.165923

analytic continuation of coupling constants of finite rank potentials with the powerful method of Balslev-Combes classical work in [40]. The coupling constant threshold behavior for short-range two-body case is studied in detail in [41]. Regarding the applications to the actual atomic and molecular systems of practical interest, Padé representations to obtain stable resonance poles were successfully attempted for the classical Stark effect in the Hydrogen atom at large electric fields [42] or in the case of Mercury Hydride [43] for which the increased numerical accuracy was needed in order to separate among the particular S-matrix poles. The ACCC method detailed in this paper was also successfully applied to the case $^2\Pi_g$ shape resonance of acetylene anion.

8 Conclusions

In this work the classical ACCC method was extended in two directions:

- To the best of our knowledge all previous application of the ACCC method in nuclear physics used the interpolation-type of Padé approximation, i.e. the order of Padé approximation was determined by the number of data points. As a consequence only a small number of points closest to the origin was used and the information contained in the more distant points was lost. In contrast to this approach we used the statistical Padé (Padé III) approximation. In such a case we can use all data points and at the same time to keep the order of the Padé approximation low.

- A variant of the ACCC method was proposed which does not require the explicit determination of the bifurcation point. In addition it appears that this variant has a broader range of application. In principle it allows for determination of more than one resonances contrary to the ACCC method which always yields only one resonance.

Both approaches were tested on the model interaction consisting of two separable terms. One term determines the resonance the other one is used to convert the resonance to the bound state. It was shown that a "good" selection of the perturbation potential is essential. A "bad" choice may cause that the sought resonance is disconnected from the bound state region. In this case the ACCC method fails whereas the inverse ACCC method works without any problem. Last but not the least stands the fact that the present approach does not require, contrary to other methods for analytical continuation, extremely high accuracy of the input data and that to get resonance energies and widths with experimental accuracy four digits of accuracy in the input data might be sufficient.

Acknowledgments

The authors thank Pavel Brožek for help with the analytical calculation. This work was supported by the Grant Agency of the Czech Republic GAČR No. 16-17230S.

References

[1] V. I. Kukulin, V. M. Krasnopolsky, and J. Horáček, Theory of resonances: Principles and Applications. Kluwer Academic Publishers, Dordrecht/Boston/London 1988.

[2] H. Kreckel, H. Bruhns, M. Čížek, S.C.O. Glover, K.A. Miller, X. Urbain, D.W. Savin, Science **328** (2010) 69.

[3] L. Sanche, Eur. Phys. J. D **35** (2005) 367–390.

[4] R. Golser, H. Gnaser, W. Kutschera, A. Priller, P. Steier, A. Wallner, M. Čížek, J. Horáček, and W. Domcke, Phys. Rev. Letters **94** (2005) 223003.

[5] H. S. Taylor, A. U. Hazi, Phys. Rev. A **14** (1976) 2071–2074.

[6] A. U. Hazi, T. N. Rescigno, and M. Kurilla, Phys. Rev. A **23** (1981) 1089.

[7] A. U. Hazi, H. S. Taylor, Phys. Rev. A **1** (1970) 1109–1120.

[8] N. Moiseyev, Physics Reports **302** (1998) 211–293.

[9] R. A. Donelly, Int. J. Quantum. Chem. Symp. **16** (1982) 653.

[10] U. V. Riss, and H.-D. Meyer, J. Phys. B: At. Mol. Opt. Phys. **26** (1993) 4503.

[11] S. Feuerbacher, T. Sommerfeld, R. Santra, and L. S. Cederbaum, J. Chem. Phys. **118** (2003) 6188–6199.

[12] V. I. Kukulin, and V. M. Krasnopolsky, J. Phys. A: Math. Gen. **10** (1977) L33-37.

[13] V. M. Krasnopolsky, and V. I. Kukulin, Phys. Lett. A **69** (1978) 251–254.

[14] N. Tanaka, Y. Suzuki, K. Varga, Phys. Rev. C **56** (1997) 562–565.

[15] S. Aoyama, Phys. Rev. Lett. **89** (2002) 052501.

[16] Y. Funaki, H. Horiuchi, A. Tohsaki, Progress of Theor. Phys. **115** (2006) 115 –127.

[17] Yang Si-Chun, Meng Jie, and Zhou Shan-Gui, Chin. Phys. Lett. **18** (2001) 196–198.

[18] G. Cattapan, and E. Maglione, Phys. Rev. C **61** (2000) 067301.

[19] J. Horáček, P. Mach, J. Urban, Phys. Rev. A **82** (2010) 032713.

[20] P. Papp, Š. Matejčik, P. Mach, J. Urban, I. Paidarová, and J. Horáček, Chem. Phys. **418** (2013) 067301.

[21] J. Horáček, I. Paidarová, and R. Čurík, J. Phys. Chem. A **118**, 33 (2014) 6536–6541.

[22] J. Horáček, I. Paidarová, and R. Čurík, J. Chem. Phys. **143** (2015) 184102.

[23] B. Nestmann and S. D. Peyerimhoff, J. Phys. B:At. Mol. Phys. **18** (1985) 615–626.

[24] T. R. Mongan, Phys.Rev. **175** (1968) 1260.

[25] S. Klarsfeld, J. Martorell, J. A. Oteo, N. Nishimura, and D. W. L. Sprung, Nucl. Phys. A **456** (1986) 373.

[26] A. Maghari, and N. Tahmasbi, J. Phys. A: Math. Gen. **38** (2005) 4469; N. Tahmasbi, and A. Maghari, Physica A **382** (2007) 537.

[27] A. J. F. Siegert, Phys. Rev. **56** (1939) 750.

[28] L. P. Kok, and H. van Haeringen, Annals of Physics **131** (1981) 426–450.

[29] G. A. Baker, and P. Graves-Morris, Padé approximants. Addison-Wesley Publishing Co., 1981.

[30] V. M. Krasnopolsky, V. I. Kukulin and J. Horáček: Czech. J. Phys. B **35** (1985) 805–819.

[31] V. M. Krasnopolsky, V. I. Kukulin and J. Horáček: Czech. J. Phys. B **40** (1990) 945–1064.

[32] J. Horáček, L. Zejda and N. M. Queen: Comp. Phys. Comm. **74** (1993) 187. Comparative Study of Methods for the Construction of Padé Approximants of Type III.

[33] S. A. Rakityanski, S. A. Sofianos, and N. Elander, J. Phys. A: Math. Theor. **40** (2007) 14857–14869.

[34] V. M. Krasnopolsky, V. I. Kukulin and J. Horáček: Czech. J. Phys. B **39** (1989) 593–613.

[35] V. M. Krasnopolsky, V. I. Kukulin, E. V. Kuznetsova, J. Horáček, and N. M. Queen, Phys. Rev. C **43** (1991) 822–834.

[36] J. S.-Y. Chao, M. F. Falcetta, K. D. Jordan, J. Chem. Phys. **93** (1990) 1125–1135.

[37] P. Krylstedt, M. Rittby, N. Elander, and E. Brändas, J. Phys. B: At. Mol. Opt. Phys. **20** (1987) 1295–1327.

[38] M. Rittby, N. Elander and E. Brändas, Lecture Notes in Physics **325** (1989) 129–151.
[39] B. Simon, Ann. Math. **97** (1973) 247–274.
[40] E. Balslev and J. M. Combes, Commun. Math. Phys. **22** (1971) 280–294.
[41] M. Klaus and B. Simon, Annals of Physics **13** (1980) 251–281.
[42] M. Hehenberger, H. McIntosh and E. Brändas, Phys. Rev. A **10** (1974) 1494 –1506.
[43] M. Hehenberger, P. Froelich and Brändas, J. Chem. Phys. **65** (1976) 4571.
[44] R. Čurík, I. Paidarová and Jiří Horáček, Eur. Phys. J. D **70** (2016) 146.